An improved Finite Fracture Mechanics approach to blunt V-notch brittle fracture mechanics: Experimental verification on ceramic, metallic, and plastic materials

CrossMark

Alberto Sapora [a,*], Pietro Cornetti [a], Alberto Carpinteri [a], Donato Firrao [b]

[a] Department of Structural, Building and Geotechnical Engineering, Politecnico di Torino, Corso Duca degli Abruzzi 24, 10129 Torino, Italy
[b] Department of Applied Science and Technology, Politecnico di Torino, Corso Duca degli Abruzzi 24, 10129 Torino, Italy

ARTICLE INFO

ABSTRACT

The coupled Finite Fracture Mechanics (FFM) criterion is applied to investigate brittle fracture in rounded V-notched samples under mode I loading. The approach is based on the contemporaneous fulfilment of a stress requirement and the energy balance, the latter being implemented on the basis of a recently proposed analytical expression for the stress intensity factor. Results are presented in terms of the critical crack advance and the apparent generalized fracture toughness, i.e. the unknowns related to the system of two equations describing the FFM criterion. A validation of the theory is performed by employing varying root radius notched, as-quenched from 1200 °C, AISI 4340 steel specimens fracture results as well as alumina and PMMA notched samples fracture results.

© 2015 Elsevier Ltd. All rights reserved.

1. Introduction

Several approaches have been successfully proposed to investigate the mode I brittle fracture of structural components containing rounded V-notches [1–7]. The basic idea of these criteria is that failure takes place when the (punctual or averaged) stress or an energy-related quantity at a finite distance from the notch tip reaches a critical value: such a distance results to be a material constant.

The critical distance becomes a structural parameter if the stress and energy conditions are coupled one to each other, as it happens for both Leguillon's criterion and FFM [8–12]: whereas the former involves a punctual stress requirement, the latter is of an average type. The coupled criteria were introduced to remove some inconsistencies related to approaches based either on stress or on energy requirements [13].

Indeed, the stress condition can be easily implemented, since an accurate expression for the stress field along the blunt notch bisector was derived [14]. This allows to develop stress-based criteria [2,3,6] in a quasi-analytical way. On the other hand, as it regards the energy balance, the relationships proposed for the stress intensity factor (SIF) related to a crack stemming from a blunt V-notch tip (providing the crack driving force) are usually approximated.

Although closed-form solutions can be obtained, the results are affected by some notch amplitude depending errors, the entity of which has to be discussed case-by-case [11]. An alternative way may consist in proceeding numerically, via a specific finite element analysis [1,9,10]. Of course, this implies a more laborious computation, since it is necessary to carry out a different simulation for each data set. Similar considerations hold for the finite-volume-energy based approach [4].

As it concerns approximating functions for the SIF of a crack stemming from a blunt V-notch, let us mention Lukas's formula [15] providing an approximating function for the SIF of a crack emanating from an elliptical hole. A U-notch can be considered as a limit case of an elliptical hole (see also [16]), when the minor axis to major axis length ratio tends to zero; upon observing that no significant deviations are generally expected for opening angles ω ($0° \leqslant \omega \leqslant 90°$), Lukas' formula can be implemented [5–12], despite its range of validity is very limited. An analytical relationship for the SIF related to a rounded V-notch was further proposed to fulfil the asymptotic limits of very short/long cracks [11]. It was numerically verified for $\omega = 90°$, 120°, and 150°, showing the maximum deviation (nearly 7%) at $\omega = 90°$. Since the energy available for a crack length increment is proportional to the integral of the squared SIF, the global error is expected to increase. Even more recently, the relationship was improved by adding a notch amplitude parameter m, the value of which was fitted by means of *ad hoc* numerical simulations [17]: in this case, the error on the SIF was estimated to be lower than 1% over the whole range

* Corresponding author.
 E-mail address: alberto.sapora@polito.it (A. Sapora).

$0° \leqslant \omega \leqslant 180°$, which can be considered very satisfying for practical applications.

The relationship provided in [17] is hereby exploited to enhance the FFM approach. The criterion, introduced in Section 2, consists in a system of two equations (one for the stress requirement and the other for the energy balance, respectively) in two unknowns: the apparent generalized fracture toughness (i.e., the failure load) and the critical crack advance. As already hinted, the latter, which coincides with the critical distance, results to be a structural parameter, controlled by the notch amplitude and the root radius, as well as by the material properties. Dimensionless results are presented in Section 3, together with the comparison with experimental data [6,18–20].

It has to be noted, that FFM has been already applied to the specific case of U-notches [12] by implementing Lukas' formula and to the general framework of structures containing blunt V-notches [11]. The novelties of the present work with respect to the past ones are substantially two: (i) the FFM implementation via the relationship proposed in [17], what allows to improve the prediction accuracy, especially on samples with smaller notch amplitudes, as well as to develop a unified FFM approach in the framework of blunt V-notches. Indeed, since the crack driving function cannot be integrated explicitly, numerical quadrature formulae must be implemented; (ii) the comparison of FFM results with various experimental data sets, covering the whole $0° \leqslant \omega \leqslant 150°$ range.

2. The Finite Fracture Mechanics criterion

The FFM approach is based on the hypothesis of a finite crack advancement l and assumes the contemporaneous fulfilment of two conditions [21,22]. By referring to the coordinate system displayed in Fig. 1a, the criterion can be expressed as:

$$\begin{cases} \int_0^l \sigma_y(x)dx \geqslant \sigma_u l \\ \int_0^l G(c)dc \geqslant G_c l \end{cases} \tag{1}$$

The former condition requires that the average stress $\sigma_y(x)$ upon the crack advancement l is higher than the material tensile strength σ_u. The latter one ensures that the energy available for a crack length increment l (involving the integration of the crack driving force G over such a length) is higher than the energy necessary to create the new fracture surfaces, $G_c l$. By means of Irwin's formula, expression (1) can be recast, at the critical mode I point, in the following form:

$$\begin{cases} \int_0^{l_c} \sigma_y(x)dx = \sigma_u l_c \\ \int_0^{l_c} K_I^2(c)dc = K_{Ic}^2 l_c \end{cases} \tag{2}$$

$K_I(c)$ and K_{Ic} being the SIFs related to a crack of length c stemming from the notch root (Fig. 1b) and the fracture toughness, respectively. A system of two equations in two unknowns is obtained, with the unknowns being the critical crack advancement and the failure load (implicitly embedded in the stress field and SIF functions). Note that, upon passing from (1) to (2), the hypothesis of positive geometries (monotonic increasing $K_I(c)$ functions) has been

implicitly assumed, allowing one to substitute the inequalities with the corresponding equalities. Furthermore, the Young's modulus of the material does not appear in the second equation of (2), since it simplifies at both sides of the expression.

In Fig. 1 the distance between the notch tip and the origin of the polar coordinates system is indicated as r_0:

$$r_0 = \frac{\pi - \omega}{2\pi - \omega}\rho \tag{3}$$

where ρ is the notch root radius.

For sharp cracks, the origin coincides with the notch root end whatever the value of ω. As the crack becomes blunter, r_0, which is also the distance between the Cartesian and polar coordinate systems origins, increases for a given value of ω. Conversely, it decreases as the notch amplitude increases for a given value of notch root radius.

2.1. The stress field

By assuming that the notch tip radius ρ is sufficiently small in respect to the notch depth a, the stress field along the notch bisector could be expressed in polar coordinates as [14]:

$$\sigma_\theta(r,0) = \frac{K_I^V}{(2\pi r)^{1-\lambda}}\left[1 + \left(\frac{r_0}{r}\right)^{\lambda-\mu}\eta_\theta(0)\right] \tag{4}$$

where K_I^V is the generalized stress intensity factor referring to a V-notch of depth a.

The eigenvalues λ and μ, as well as the function $\eta_\theta(0)$, depend on the notch amplitude ω. These latter three parameters are reported in Fig. 2.

2.2. The SIF function

Let us consider a crack of length c stemming from a blunted V-notch root (Fig. 1b). As far as the notch depth a is sufficiently large with respect to c, the following SIF function was proposed [17],

$$K_I(c) = \frac{K_I^V \beta c^{\lambda-1/2}}{\left\{1 + \left[\left(\frac{\beta}{\psi}\right)^{\frac{1}{1-\lambda}}\frac{r_0}{c}\right]^m\right\}^{\frac{1-\lambda}{m}}} \tag{5}$$

The notch angle amplitude functions β and m are drawn in Fig. 2; ψ is equal to $1.12\sqrt{\pi}\,(1 + \eta_\theta(0))\,(2\pi)^{\lambda-1}$. Note that the parameter m was fitted to improve the predictions obtained by carrying out an *ad hoc* finite element analysis [17]: Eq. (5) fulfils the asymptotic limits of very short and very long (but still small in respect to the notch depth) cracks, providing errors below 1%, for $0 \leqslant c/\rho \leqslant 10$ and over the range $0° \leqslant \omega \leqslant 180°$.

3. FFM implementation

By hypothesizing that failure takes place when the generalized SIF K_I^V, reaches its critical conditions $K_{Ic}^{V,\rho}$, as expected for brittle structural behaviour, FFM can be implemented by inserting
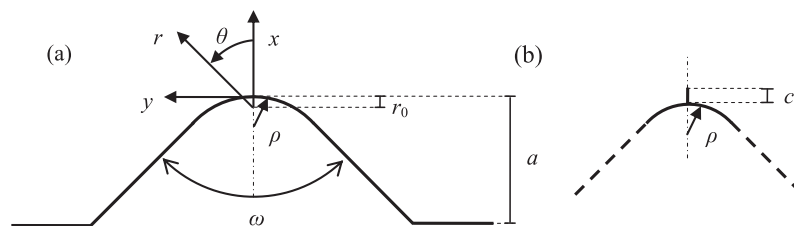

Fig. 1. (a) Blunt V-notch with Cartesian and polar coordinate systems and (b) crack of length c stemming from the notch tip.
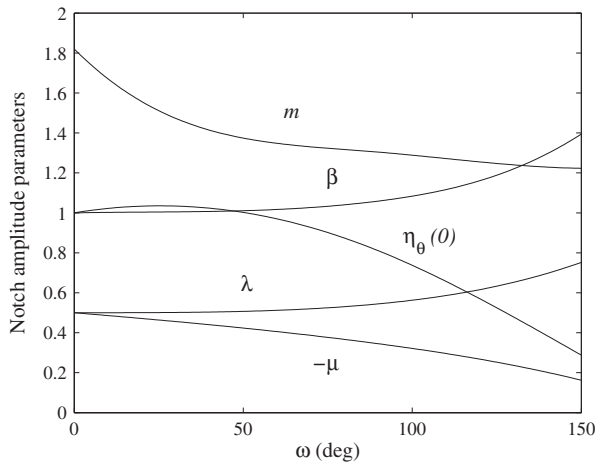
Fig. 2. Notch angle amplitude dependent parameters used in the present analysis.

Fig. 3. Dimensionless plot of the critical crack advancement vs notch root radius according to FFM.

Eqs. (4) and (5) into system (2) and integrating. Note that $K_{Ic}^{V,\rho}$ represents the apparent generalized fracture toughness (i.e. the generalized fracture toughness measured as if the V-notch was sharp): it depends on the root radius, differently from the generalized SIF, K_I^V. Some analytical manipulations yield:

$$\begin{cases} \dfrac{K_{Ic}^{V,\rho}}{\sigma_u r_0^{1-\lambda}} = f(\bar{l}_c), \\[2mm] \dfrac{K_{Ic}^{V,\rho}}{K_{Ic} r_0^{1/2-\lambda}} = \sqrt{h(\bar{l}_c)}, \end{cases} \qquad (6)$$

where

$$f(\bar{l}_c) = \frac{(2\pi)^{1-\lambda}\bar{l}_c}{\left[\dfrac{(\bar{l}_c+1)^{\lambda}-1}{\lambda}\right] + \eta_\theta(0)\left[\dfrac{(\bar{l}_c+1)^{\mu}-1}{\mu}\right]}, \qquad (7a)$$

$$h(\bar{l}_c) = \frac{\bar{l}_c}{\displaystyle\int_0^{\bar{l}_c} \frac{\beta^2 \bar{c}^{2\lambda-1}}{\left\{1 + \left[\left(\dfrac{\beta}{\psi}\right)^{\frac{1}{1-\lambda}}\dfrac{1}{\bar{c}}\right]^m\right\}^{\frac{2(1-\lambda)}{m}}} d\bar{c}}, \qquad (7b)$$

$\bar{l}_c = l_c/r_0$ and $\bar{c} = c/r_0$.

Note that the presence of the parameter m in Eq. (7b) does not allow to get a closed form solution for function h: the integral will be thus evaluated numerically according to a recursive adaptive Simpson quadrature formula. By equaling both expressions in (6) with respect to $K_{Ic}^{V,\rho}$, the problem can be recast in the following form:

$$\begin{cases} \dfrac{K_{Ic}^{V,\rho}}{\sigma_u r_0^{1-\lambda}} = f(\bar{l}_c), \\[2mm] \dfrac{r_0}{l_{ch}} = \dfrac{h(\bar{l}_c)}{f^2(\bar{l}_c)}, \end{cases} \qquad (8)$$

where $l_{ch} = (K_{Ic}/\sigma_u)^2$ is the Irwin's length. For a given material, notch amplitude ω and notch root radius ρ, the estimate of the critical crack advancement $\bar{l}_c$ can be derived from the second equation in (8). This value must then be inserted into the former equation to obtain the apparent generalized fracture toughness, $K_{Ic}^{V,\rho}$.

FFM results are presented in Figs. 3 and 4 in dimensionless form as compared to the sharp V-notch case, according to which [13]:
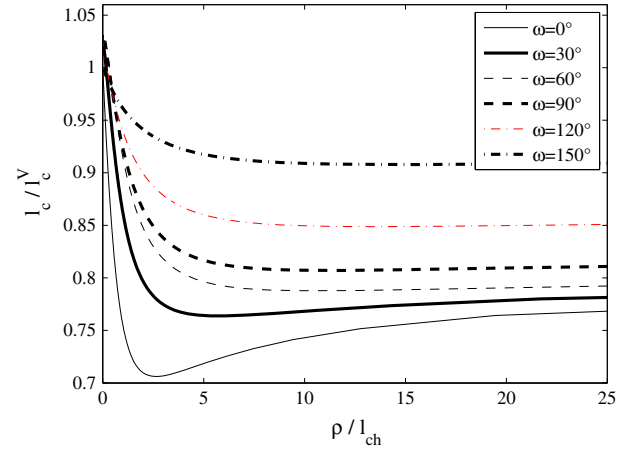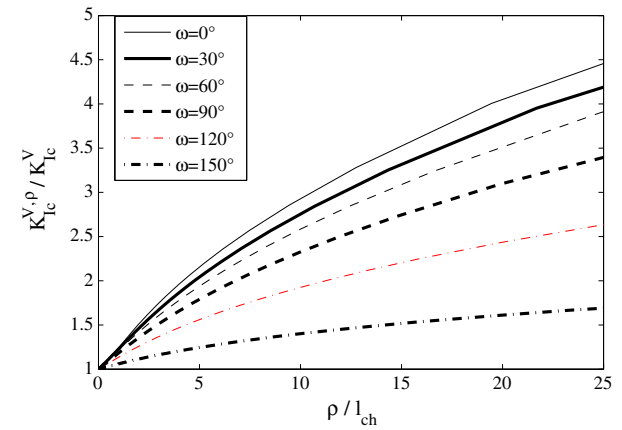

Fig. 4. Dimensionless plot of the apparent generalized fracture toughness vs. notch root radius according to FFM.

$$l_c^V = \frac{2}{\lambda\beta^2(2\pi)^{2(1-\lambda)}} l_{ch}, \qquad (9a)$$

$$K_{Ic}^V = \lambda^\lambda \left[\frac{2(2\pi)^{2\lambda-1}}{\beta^2}\right]^{1-\lambda} l_{ch}^{1-\lambda}\sigma_u. \qquad (9b)$$
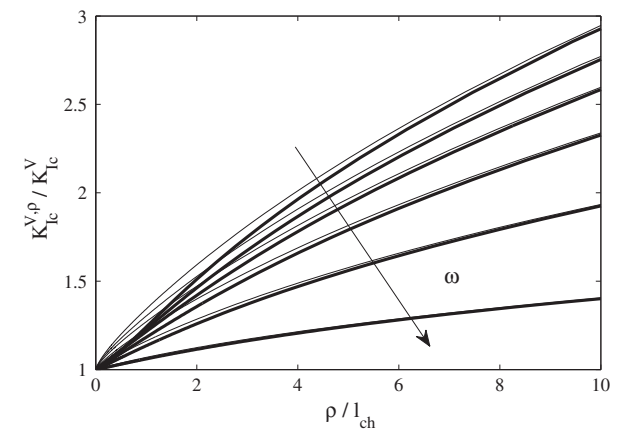

Fig. 5. Different FFM predictions for the dimensionless apparent generalized fracture toughness: the thin lines describes the results obtained in [11], the thick lines are related to the present improved approach. From top to bottom, curves refer to $\omega = 0°$, 30°, 60°, 90°, 120° and 150°.

In Fig. 5 the apparent generalized fracture toughness is reported according to the present FFM approach and to the one proposed in [11], obtained simply by setting $m = 1$ in Eq. (5). Note that the maximum deviations (and consequently the most significant improvements) are observed for lower root radii and lower notch angle amplitudes ω, as expected since m decreases as ω increases.

3.1. Comparison with experimental data

Let us now compare FFM predictions with experimental data available in the Literature: different materials, root radii and notch amplitudes are taken into account.

The firstly considered data set refers to three point bending tests on single edge U-notched specimens made of alumina [20]. The material properties are $K_{Ic} = 3.81$ MPa $\sqrt{m}$ and $\sigma_u = 290$ MPa, corresponding to $l_{ch} \sim 0.173$ mm. FFM predictions, in terms of the apparent fracture toughness $K_{Ic}^U = K_{Ic}^{V=0,\rho}$ are plotted in Fig. 6, showing a very good matching. The calibration of the parameter m in Eq. (5) allows to get a more flat behaviour in the neighbourhood of $\rho = 0$ with respect to the FFM approach put forward in [11]. Note that the presence of a minimum was highlighted in [7] by implementing some criteria based on a critical distance.

The second data set taken into account is related to Charpy V notch specimens fabricated with as quenched AISI 4340 steel: they were heat treated by a 1200–870 °C step quenching procedure and tested under three-point bending. Although the V-notch angle related to Charpy samples is 45°, it was considered as a crack ($\omega = 0°$) in [18,19]. The measured AISI 4340 steel properties are: $K_{Ic} = 73.9$ MPa $\sqrt{m}$ and $\sigma_u = 1980$ MPa, resulting in $l_{ch} \sim 1.39$ mm. The material is of course less brittle than common ceramic materials, usually tested to investigate blunt V-notch brittle fracture. Indeed, it has been shown that some criteria, such as the point-stress approach, work rather well even for ductile metallic materials, when the final rupture is preceded by large-scale plastic deformations [23]. FFM results are shown in Fig. 7: predictions are acceptable except for the largest root radii ($\rho \geqslant 0.6$ mm) where the percent deviation grows up to nearly 27% for $\rho = 2.0$ mm. In these cases the radius is not negligible with respect to the notch depth ($a = 2$ mm): higher order terms must be taken into account in the asymptotic expansions (4) and (5) to improve FFM accuracy.

Eventually, in order to face cases where $\omega > 0°$, we consider the rounded-tip semi-circular bend specimens tested in [6]. The

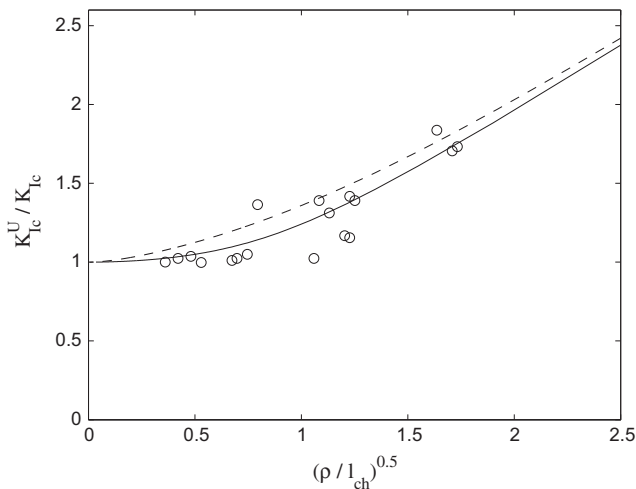**Fig. 7.** Dimensionless apparent fracture toughness versus dimensionless square root of the notch root radius according to FFM (continuous line): experimental data (circles) refer to as – quenched AISI 4340 steel [18].

Fig. 8. FFM failure predictions on PMMA blunted V-notched samples [6] referring to $\omega = 30°$: theoretical results (continuous line) and experimental data (circles).

Fig. 6. Dimensionless apparent fracture toughness versus dimensionless square root of the notch root radius according to FFM (continuous line): experimental data (circles) refer to alumina [20]. The dotted line refers to the model presented in [11].
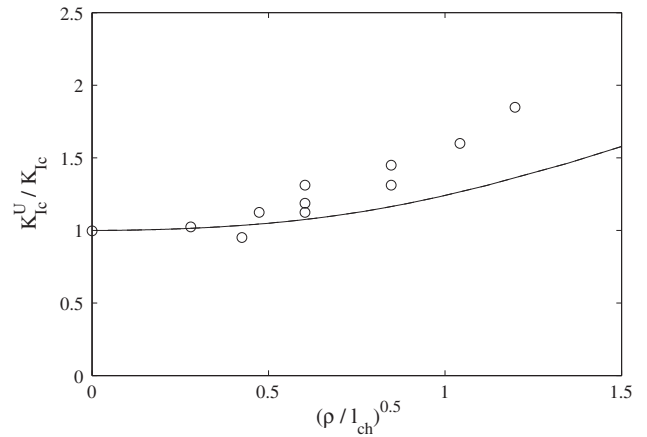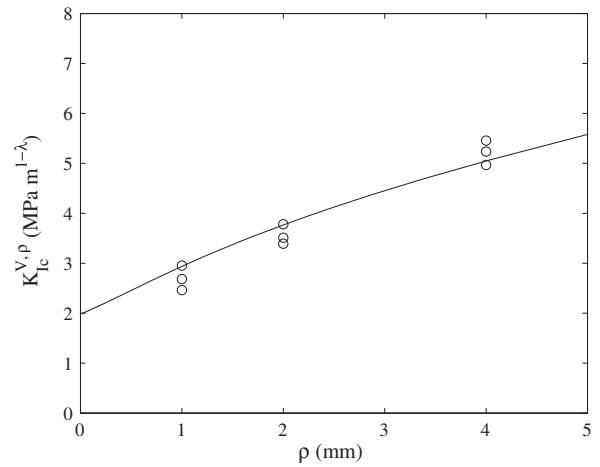

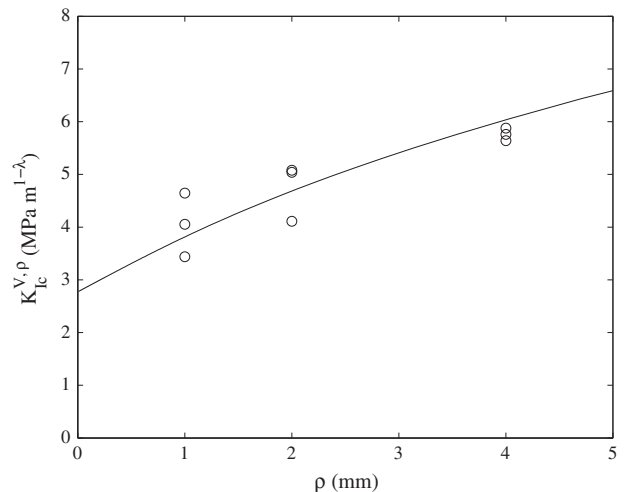**Fig. 9.** FFM failure predictions on PMMA blunted V-notched samples [6] referring to $\omega = 90°$: theoretical results (continuous line) and experimental data (circles).
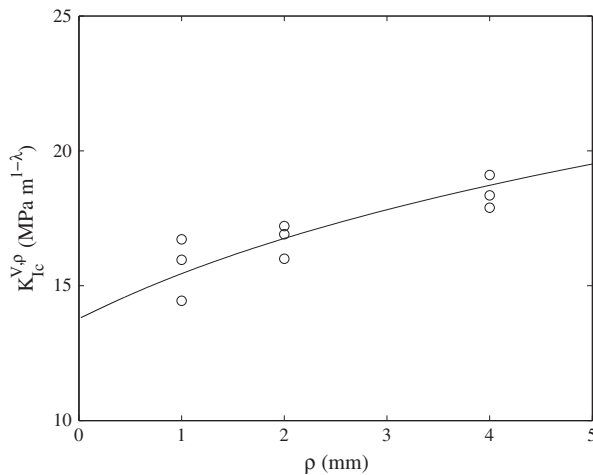
Fig. 10. FFM failure predictions on PMMA blunted V-notched samples [6] referring to $\omega = 150°$: theoretical results (continuous line) and experimental data (circles).

material is PMMA, with the following measured properties: $K_{Ic} = 1.96$ MPa $\sqrt{m}$, $\sigma_u = 70.5$ MPa. Indeed, as observed in [24], the value of σ_u to be used is not the tensile strength obtained by testing plain specimens, since this last quantity can be strongly affected by the presence of micro-cracks/defects or crazing phenomena. As a matter of fact, σ_u has to be fitted and may be equal to even twice the one related to plain specimens.

In the present work, we assume $\sigma_u = 90$ MPa, this value being fitted on FFM predictions. As a result, we have $l_{ch} \sim 0.474$ mm. Results are presented in Figs. 8–10 for what concerns $\omega = 30°$, $90°$, and $150°$. The agreement is satisfactory for all the considered cases.

4. Conclusions

The novel expression for the SIF related to a crack stemming from a blunted V-notch proposed in [17] allows us to improve FFM predictions on mode I brittle fracture. Results are in good agreement with experimental data rising from different tests and different materials. The analysis is valid over the whole range $0° \leqslant \omega \leqslant 180°$ and covers a wide range of notch radii and materials, useful for different practical applications. As a future development, the next step will consist in investigating the effects of the root radius on mixed-mode brittle fracture: note that some criteria have already been successfully proposed [25,26] and some considerations have been already pointed out also through FFM [27,28], although the direct implementation of the present approach in this framework is still missing.

References

[1] F.J. Gomez, M. Elices, A fracture criterion for blunted V-notched samples, Int. J. Fract. 127 (2004) 239–264.

[2] D. Taylor, Predicting the fracture strength of ceramic materials using the theory of critical distances, Eng. Fract. Mech. 71 (2004) 2407–2416.

[3] N. Pugno, B. Peng, H.D. Espinosa, Predictions of strength in MEMS components width defects – a novel experimental theoretical approach, Int. J. Solids Struct. 42 (2004) 647–661.

[4] P. Lazzarin, F. Berto, Some expressions for the strain energy in a finite volume surrounding the root of blunted V-notches, Int. J. Fract. 135 (2005) 161–185.

[5] F.J. Gomez, G.V. Guinea, M. Elices, Failure criteria for linear elastic materials with U-notches, Int. J. Fract. 141 (2006) 99–113.

[6] M.R. Ayatollahi, A.R. Torabi, Brittle fracture in rounded-tip V-shaped notches, Mater. Des. 31 (2010) 60–67.

[7] E. Barati, Y. Alizadeh, A notch root radius to attain minimum fracture loads in plates weakened by U-notches under mode I loading, Sci. Iran. 19 (2012) 491–502.

[8] D. Leguillon, Z. Yosibash, Crack onset at a V-notch: influence of the notch tip radius, Int. J. Fract. 122 (2003) 1–21.

[9] Z. Yosibash, A. Bussiba, I. Gilad, Failure criteria for brittle elastic materials, Int. J. Fract. 125 (2004) 307–333.

[10] D. Picard, D. Leguillon, C. Putot, A method to estimate the influence of the notch-root radius on the fracture toughness of ceramics, J. Eur. Ceram. Soc. 26 (2006) 1421–1427.

[11] A. Carpinteri, P. Cornetti, A. Sapora, Brittle failures at rounded V-notches: a finite fracture mechanics approach, Int. J. Fract. 172 (2011) 1–8.

[12] A. Carpinteri, P. Cornetti, A. Sapora, A finite fracture mechanics approach to the asymptotic behavior of U-notched structures, Fatigue Fract. Eng. Mater. Struct. 35 (2012) 451–457.

[13] A. Carpinteri, P. Cornetti, N. Pugno, A. Sapora, D. Taylor, A finite fracture mechanics approach to structures with sharp V-notches, Eng. Fract. Mech. 75 (2008) 1736–1752.

[14] S. Filippi, P. Lazzarin, R. Tovo, Developments of some explicit formulas useful to describe elastic stress fields ahead of notches in plates, Int. J. Solid Struct. 39 (2002) 4543–4565.

[15] P. Lukas, Stress intensity factor for small notch-emanated cracks, Eng. Fract. Mech. 26 (1987) 471–473.

[16] R.X. Xu, J.C. Thompson, T.H. Topper, Practical stress expressions for stress concentration regions, Fatigue Fract. Eng. Mater. Struct. 22 (1995) 885–895.

[17] A. Sapora, P. Cornetti, A. Carpinteri, Cracks at rounded V-notch tips: an analytical expression for the stress intensity factor, Int. J. Fract. 187 (2014) 285–291.

[18] R. Roberti, G. Silva, B. De Benedetti, D. Firrao, The influence of high temperature austenitization on the toughness properties of as-quenched AISI 4340 steel, Metall. Ital. 70 (1978) 449–455.

[19] D. Firrao, J.A. Begley, G. Silva, R. Roberti, B. De Benedetti, The influence of notch root radius and austenitizing temperature on fracture appearance of as-quenched Charpy-V type AISI 4340 steel specimens, Metall. Trans. A 13A (1982) 1003–1013.

[20] K. Tsuji, K. Iwase, K. Ando, An investigation into the location of crack initiation sites in alumina, polycarbonate and mild steel, Fatigue Fract. Eng. Mater. Struct. 22 (1999) 509–517.

[21] P. Cornetti, N. Pugno, A. Carpinteri, D. Taylor, Finite fracture mechanics: a coupled stress and energy failure criterion, Eng. Fract. Mech. 73 (2006) 2021–2033.

[22] A. Carpinteri, P. Cornetti, N. Pugno, A. Sapora, D. Taylor, Generalized fracture toughness for specimens with re-entrant corners: experiments vs. theoretical predictions, Struct. Eng. Mech. 32 (2009) 609–620.

[23] L. Susmel, D. Taylor, On the use of the theory of critical distances to predict static failures in ductile metallic materials containing different geometrical features, Eng. Fract. Mech. 75 (2008) 4410–4421.

[24] D. Taylor, P. Cornetti, N. Pugno, The fracture mechanics of finite crack extension, Eng. Fract. Mech. 72 (2005) 1021–1038.

[25] M.R. Ayatollahi, F. Berto, P. Lazzarin, Mixed mode brittle fracture of sharp and blunt V-notches in polycristalline graphite, Carbon 49 (2011) 2465–2474.

[26] F. Berto, P. Lazzarin, C. Marangon, Brittle fracture of U-notched graphite plates under mixed mode loading, Mater. Des. 41 (2012) 421–432.

[27] E. Priel, Z. Yosibash, D. Leguillon, Failure initiation at a blunt V-notch tip under mixed mode loading, Int. J. Fract. 149 (2008) 143–173.

[28] A. Sapora, P. Cornetti, A. Carpinteri, A finite fracture mechanics approach to V-notched elements subjected to mixed-mode loading, Eng. Fract. Mech. 97 (2013) 216–226.